PROBING INITIAL- AND FINAL-STATE EFFECTS OF HEAVY-ION COLLISIONS WITH STAR EXPERIMENT*

Gaoguo Yan

for the STAR Collaboration

Institute of Frontier and Interdisciplinary Science, Shandong University
Qingdao, Shandong, 266237, China

Received 30 July 2022, accepted 19 September 2022, published online 14 December 2022

Measurements of longitudinal flow decorrelation for charged particles in Zr+Zr and Ru+Ru (isobar) collisions at $\sqrt{s_{NN}} = 200$ GeV and Au+Au collisions at $\sqrt{s_{NN}} = 19.6$, 27 and 54.4 GeV using the STAR detector are presented. The third-order flow decorrelation is stronger than the second order one. The second-order flow decorrelation shows a strong centrality dependence, while the third-order results show a weak dependence. Comparing with Au+Au collisions at $\sqrt{s_{NN}} = 27$ and 54.4 GeV, both the second- and third-order flow decorrelations show obvious energy dependence. In addition, the correlation coefficient $\rho(v_n^2, [p_T])$ is also measured in Au+Au collisions at $\sqrt{s_{NN}} = 19.6$–200 GeV. No obvious energy dependence is observed for $\rho(v_n^2, [p_T])$. These results provide significant constraints on the initial-state fluctuations.

DOI:10.5506/APhysPolBSupp.16.1-A137

1. Introduction

Heavy-ion collisions create a strongly coupled, hot and dense medium known as a quark–gluon plasma (QGP) whose space-time evolution is described by relativistic viscous hydrodynamic models. During its dynamical evolution, the spatial anisotropy in the initial-state geometry can transform into the momentum anisotropy of the final-state particles due to large pressure gradients. This anisotropy of final-state particles can be characterized by the Fourier expansion of final particles yield distribution in azimuthal angle, $\mathrm{d}N/\mathrm{d}\phi \propto 1+2\sum_n v_n \cos[n(\phi-\psi_n)]$, where v_n and ψ_n are the magnitude and phase angle of anisotropic flow. In the early days of flow studies, we

* Presented at the 29th International Conference on Ultrarelativistic Nucleus–Nucleus Collisions: Quark Matter 2022, Kraków, Poland, 4–10 April, 2022.

usually assume that the initial state is smooth and flow is boost-invariant. However, initial-state fluctuations play an important role, for example, the fluctuations of nucleon positions.

Recently, both theoretical models [1–3] and experiments [4, 5] show that v_n and ψ_n can fluctuate along the longitudinal direction. Such decorrelation effects can be characterized by the factorization ratio $r_n(\eta)$ [4].

$$r_n(\eta) = \frac{\langle q_n(-\eta) q_n^*(\eta_{\rm ref})\rangle}{\langle q_n(\eta) q_n^*(\eta_{\rm ref})\rangle} = \frac{\langle v_n(-\eta) v_n(\eta_{\rm ref}) \cos\{n[\psi_n(-\eta) - \psi_n(\eta_{\rm ref})]\}\rangle}{\langle v_n(\eta) v_n(\eta_{\rm ref}) \cos\{n[\psi_n(\eta) - \psi_n(\eta_{\rm ref})]\}\rangle}, \quad (1)$$

where $\langle ... \rangle$ indicates an average over all events, $q_n(\eta)$ and $q_n(-\eta)$ are constructed from charged tracks measured in the Time Projection Chamber (TPC, $|\eta| < 1.0$) and $q_n(\eta_{\rm ref})$ is constructed from the Event Plane Detector (EPD, $2.1 < |\eta_{\rm ref}| < 5.1$). The $r_n(\eta)$ measures relative fluctuations between forward ($+\eta$ range) and backward ($-\eta$ range) rapidities. In these proceedings, we present flow decorrelation results in Zr+Zr and Ru+Ru collisions at $\sqrt{s_{NN}} = 200$ GeV and Au+Au collisions at $\sqrt{s_{NN}} = 19.6$, 27, and 54.4 GeV using the STAR detector to explore the system size and energy dependence. The charged particles are required to have transverse momentum, $0.4 < p_{\rm T} < 4.0$ GeV/c and pseudorapidity range, $|\eta| < 1.0$, except for 19.6 GeV with $|\eta| < 1.5$ because of using the inner Time Projection Chamber (iTPC). The systematic uncertainties are evaluated by using negative and positive tracks separately, and by varying track selections.

The shape and size of initial-state fluctuations can contribute to the higher harmonics (v_n for $n = 3, 4, \dots$) and to the fluctuation of mean transverse momentum [$p_{\rm T}$] of the final-state particles, respectively. The v_n–[$p_{\rm T}$] correlation can probe the correlation between shape and size in the initial state. The Pearson correlation coefficient (PCC) [6] is used to indicate the strength of v_n–[$p_{\rm T}$] correlation

$$\rho\left(v_n^2, [p_{\rm T}]\right) = \frac{{\rm cov}\left(v_n^2, [p_{\rm T}]\right)}{\sqrt{{\rm var}\left(v_n^2\right)}\sqrt{{\rm var}\left([p_{\rm T}]\right)}}, \quad (2)$$

where cov(v_n^2, [$p_{\rm T}$]) is the covariance between v_n^2 and [$p_{\rm T}$], and var(v_n^2) and var([$p_{\rm T}$]) are the variances of the v_n^2 and [$p_{\rm T}$] distributions, respectively. Experimental results can provide important constraints on models with the initial-state conditions [7]. In these proceedings, we also present v_n–[$p_{\rm T}$] correlation results in Au+Au collisions at $\sqrt{s_{NN}} = 19.6$, 27, 54.4, and 200 GeV to probe its beam energies dependence.

2. Results and discussions

Figures 1 and 2 show the $r_n(\eta)$ for $n = 2, 3$ in Zr+Zr and Ru+Ru collisions at $\sqrt{s_{NN}} = 200$ GeV in 0–10%, 10–40%, and 40–80% centralities. The $r_n(\eta)$ results between Zr+Zr and Ru+Ru collisions are consistent within uncertainties. The value of $r_n(\eta)$ decreases linearly with increasing η. The values of $r_3(\eta)$ are smaller than $r_2(\eta)$, implying a stronger flow decorrelation for higher-order harmonics. The second-order flow decorrelation becomes weak first and then strong as we move from central to peripheral collisions. Such a dependence is the result of a strong centrality dependence of v_2 which is dominated by initial elliptic geometry. On the other hand, no obvious centrality dependence for the third-order flow decorrelation is observed since the third-order flow is driven by the initial fluctuations.

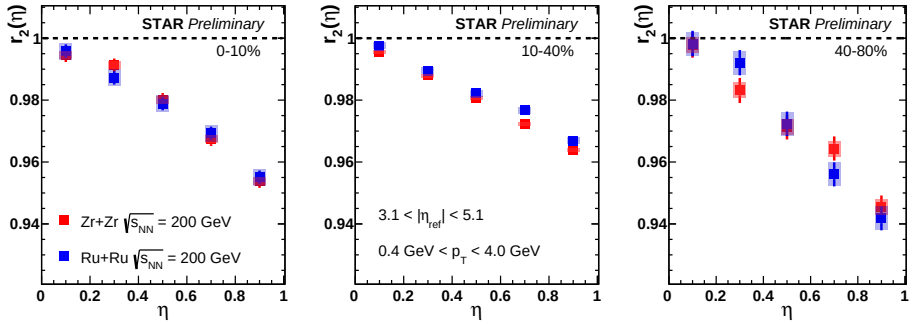

Fig. 1. (Colour on-line) The factorization ratio $r_2(\eta)$ in Zr+Zr (gray/red squares) and Ru+Ru (black/blue squares) collisions at $\sqrt{s_{NN}} = 200$ GeV in three centralities. The error bars and shaded boxes represent statistical and systematic uncertainties, respectively.

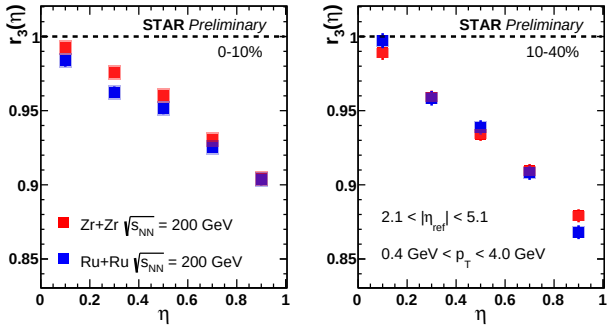

Fig. 2. (Colour on-line) The factorization ratio $r_3(\eta)$ in Zr+Zr (gray/red squares) and Ru+Ru (black/blue squares) collisions at $\sqrt{s_{NN}} = 200$ GeV in two centralities. The error bars and shaded boxes represent statistical and systematic uncertainties, respectively.

Figures 3 and 4 show the $r_n(\eta)$ for $n = 2, 3$ in Au+Au collisions at $\sqrt{s_{NN}}$ = 19.6, 27, and 54.4 GeV in 0–10%, 10–40%, and 40–80% centralities. For each energy, the longitudinal flow decorrelation depends on the harmonic of the order n and collision centrality, and decreases linearly with η as observed in isobar collisions. The slope of $r_2(\eta)$ at 27 GeV is stronger than that at 54.4 GeV, indicating that lower-energy collisions have large decorrelation. This effect is similar to observations from the LHC results [5], which indicates that lower-energy collisions become less boost-invariant along the longitudinal direction. However, there is no obvious difference between 19.6 and 27 GeV which might be due to their small energy difference. No solid conclusion of energy dependence can be drawn for $r_3(\eta)$ due to the statistical limitations.

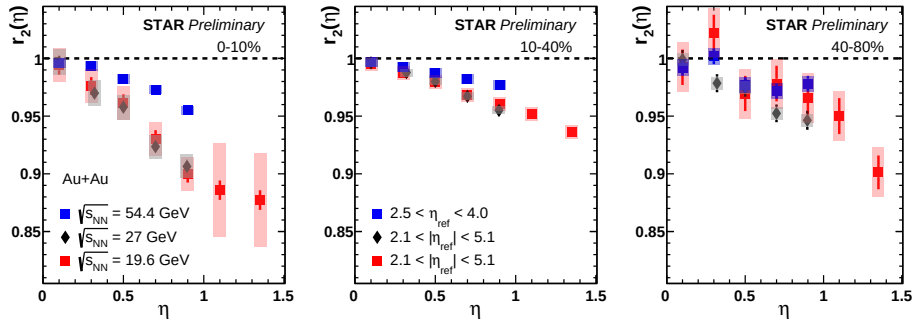

Fig. 3. The factorization ratio $r_2(\eta)$ in Au+Au collisions at $\sqrt{s_{NN}}$ = 19.6, 27, and 54.4 GeV in three centralities. The error bars and shaded boxes represent statistical and systematic uncertainties, respectively.

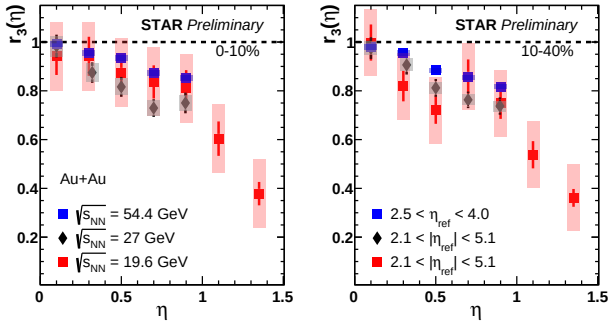

Fig. 4. The factorization ratio $r_3(\eta)$ in Au+Au collisions at $\sqrt{s_{NN}}$ = 19.6, 27, and 54.4 GeV in two centralities. The error bars and shaded boxes represent statistical and systematic uncertainties, respectively.

Figure 5 shows the beam energy dependence of var(v_2^2), c_k, cov$(v_2^2, [p_T])$, and $\rho(v_2^2, [p_T])$ in different centralities. The var$([p_T])$ is replaced c_k in Eq. (2)

where $c_k = \langle \frac{1}{N_{\rm pair}} \sum_i \sum_j (p_{\rm T}^i - \langle [p_{\rm T}] \rangle)(p_{\rm T}^j - \langle [p_{\rm T}] \rangle) \rangle$. The $\mathrm{var}(v_2^2)$, c_k, and $\mathrm{cov}(v_2^2, [p_{\rm T}])$ decrease with beam energy due to a larger contribution from the average $p_{\rm T}$ change. The $\rho(v_2^2, [p_{\rm T}])$ is sensitive to initial fluctuations and shows a hint of beam energy dependence, which indicates a stronger correlation at lower energy.

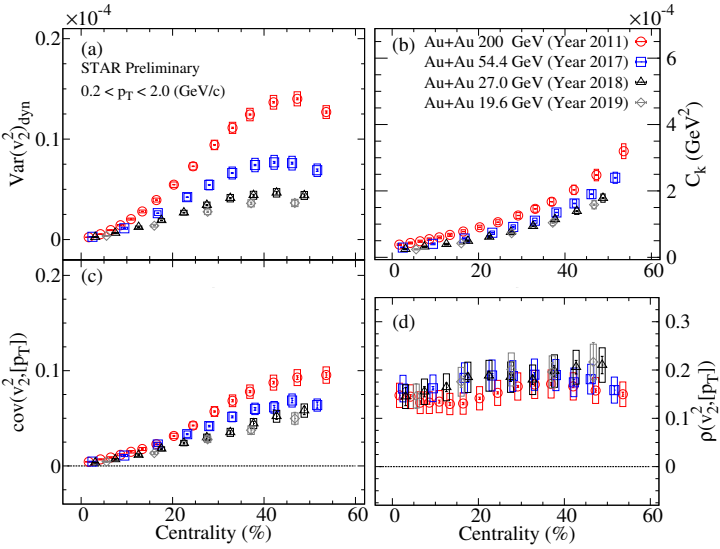

Fig. 5. The centrality dependence of $\mathrm{var}(v_2^2)$ (a), c_k (b), $\mathrm{cov}(v_2^2, [p_{\rm T}])$ (c), and $\rho(v_2^2, [p_{\rm T}])$ (d) for Au+Au collisions at $\sqrt{s_{NN}} = 19.6$, 27, 54.4, and 200 GeV.

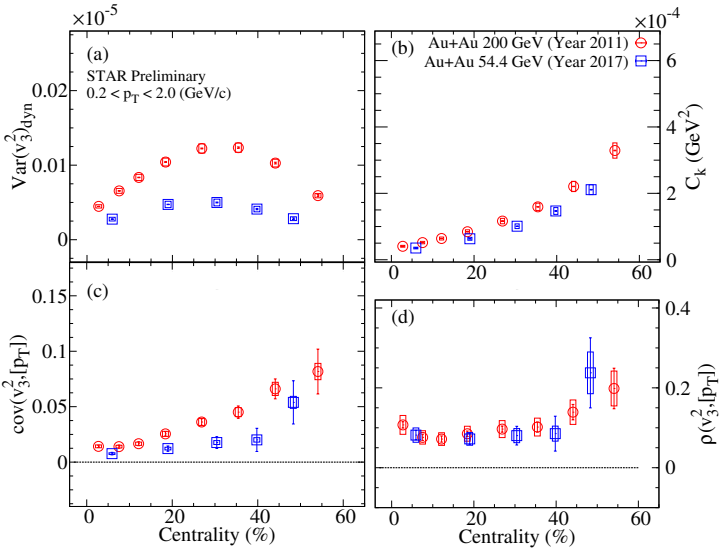

Fig. 6. The centrality dependence of $\mathrm{var}(v_3^2)$ (a), c_k (b), $\mathrm{cov}(v_3^2, [p_{\rm T}])$ (c), and $\rho(v_3^2, [p_{\rm T}])$ (d) for Au+Au collisions at $\sqrt{s_{NN}} = 54.4$ and 200 GeV.

Figure 6 compares $\mathrm{var}(v_3^2)$, c_k, $\mathrm{cov}(v_3^2, [p_\mathrm{T}])$, and $\rho(v_3^2, [p_\mathrm{T}])$ for Au+Au collisions between $\sqrt{s_{NN}} = 200$ and 54.4 GeV. Similarly, the $\mathrm{var}(v_3^2)$, c_k, and $\mathrm{cov}(v_3^2, [p_\mathrm{T}])$ decrease with beam energy. However, the $\rho(v_3^2, [p_\mathrm{T}])$ shows no clear energy dependence which demonstrates the similar initial fluctuations in $\sqrt{s_{NN}} = 200$ and 54.4 GeV.

3. Conclusion

The longitudinal flow decorrelation for charged particles was measured in Zr+Zr and Ru+Ru collisions at $\sqrt{s_{NN}} = 200$ GeV and Au+Au collisions at $\sqrt{s_{NN}} = 19.6$, 27, and 54.4 GeV. The factorization ratio $r_n(\eta)$ decreases linearly with increasing η showing that flow decorrelation is stronger at larger-η separation between the two particles. For $n = 2$, the effect is smallest in 10–40% centrality and increases in 0–10% and 40–80% centralities. For $n = 3$, there is no obvious centrality dependence. Comparisons with $\sqrt{s_{NN}} = 27$ and 54.4 GeV show strong energy dependence. In addition, the correlation coefficient $\rho(v_n^2, [p_\mathrm{T}])$ was also measured in Au+Au collisions at $\sqrt{s_{NN}} = 19.6$, 27, 54.4, and 200 GeV. No obvious energy dependence is observed for the results. These results provide new insights into the three-dimensional initial state and important input for theoretical models.

This work is supported by the National Natural Science Foundation of China under grant 12105156, project ZR2021QA084 supported by the Shandong Provincial Natural Science Foundation.

REFERENCES

[1] P. Bożek, W. Broniowski, J. Moreira, *Phys. Rev. C* **83**, 034911 (2011).
[2] J. Jia, P. Huo, *Phys. Rev. C* **90**, 034915 (2014).
[3] L.-G. Pang *et al.*, *Eur. Phys. J. A* **52**, 97 (2016).
[4] CMS Collaboration (V. Khachatryan *et al.*), *Phys. Rev. C* **92**, 034911 (2015).
[5] ATLAS Collaboration (M. Aaboud *et al.*), *Eur. Phys. J. C* **78**, 142 (2018).
[6] P. Bożek, *Phys. Rev. C* **93**, 044908 (2016).
[7] ATLAS Collaboration (G. Aad *et al.*), *Eur. Phys. J. C* **79**, 985 (2019).